International Journal of Chemical, Materials and Biomolecular Sciences
ISSN: 2415-6620
Vol:10, No:10, 2016

Predicting Depth of Penetration in Abrasive Waterjet Cutting of Polycrystalline Ceramics

S. Srinivas, N. Ramesh Babu

***Abstract*—**This paper presents a model to predict the depth of penetration in polycrystalline ceramic material cut by abrasive waterjet. The proposed model considered the interaction of cylindrical jet with target material in upper region and neglected the role of threshold velocity in lower region. The results predicted with the proposed model are validated with the experimental results obtained with Silicon Carbide (SiC) blocks.

***Keywords*—**Abrasive waterjet cutting, analytical modeling, ceramics, microcutting and intergranular cracking.

I. Introduction

MODELING of abrasive water jet cutting (AWJC) is important to analyze the performance of abrasive waterjets (AWJs) in cutting of materials and to predict material the removal rate and the depth of penetration of AWJs in the materials. Among the several approaches employed for building process models, analytical models are suitable to identify the range of process parameters with which the experimentation can be conducted. The data collected from the experimentation can be used to develop empirical models which in turn help in choosing optimal parameters for effective processing of materials.

In AWJ cutting of ceramic materials, material removal takes place due to microcutting and intergranular cracking at shallow impact angles of particles in upper zone and plastic deformation and intergranular cracking at larger angles of impact of particles in lower zone. Analytical models developed for predicting the jet penetration depths in ceramic materials are limited. A model was proposed to find volumetric MRR using Finnie's erosion model (1960) for ductile materials and therefore it neglects the effects of particle shape and size of abrasives [1]. Paul et al. (1998) opined that the material removal in ceramic materials is due to microcutting and intergranular cracking at shallow angles of impact of particles in upper zone and at larger impact angles of abrasives material removal takes place due to plastic deformation and intergranular cracking in lower zone [2]. Hashish (1989) model was modified to estimate the depth of penetration due to microcutting and plastic deformation [3]. Though the particles shape and size in predicting the depth of penetration of jet was considered, it uses planar jet interaction with the target material to estimate volumetric MRR in upper region and the jet deflecting in longitudinal direction forms a two-dimensional shaped kerf with uniform width over the entire depth. It considered the role of threshold velocity in removing the material in lower region. This model was validated up to 3 mm depth of penetration of jet. An empirical model was developed using dimensional analysis to predict depth of cut for alumina ceramics [4]. Since the analytical models to predict the depth of cut are limited, there exists a scope to develop such models.

This paper presents a model to predict the depth of penetration for AWJ cutting of polycrystalline ceramic materials considering the interaction of cylindrical jet with the target material in the upper region and neglecting the role of threshold velocity on depth of penetration of jet in lower region.

II. Methodology

The objective of the proposed model is to develop a model for predicting larger depth of penetration of jet in ceramic materials. The total depth of penetration of jet in ceramic material is sum of depths of penetration of jet in upper and lower regions. The methodology adopted in developing the present model is given as

a) Estimation of depth of penetration of jet in upper region by equating the physically obtained volumetric MRR to geometrically obtained volumetric MRR due to microcutting and intergranular cracking. While determining the volumetric MRR with the trajectory, the interaction of cylindrical shaped jet with target material is considered.
b) Estimation of depth of penetration of jet in lower region by equating the physically obtained volumetric MRR to the geometrically obtained volumetric MRR due to plastic deformation and intergranular cracking. While determining the volumetric MRR with the trajectory, the effect of threshold velocity on material removal is neglected.
c) Validation of the model developed for predicting depth of penetration of jet.

Several assumptions made in the model are i) the diameter of focusing tube is equal to top width of kerf, ii) the diameter of focusing tube is equal to diameter of jet thus, spreading of jet is ignored, iii) no particle fragmentation and iv) distribution of abrasive particles is uniform over the jet cross sectional area

S. Srinivas is with Dept. of Mechanical Engg, BMS College of Engineering, Basavanagudi, Bengaluru, Karnataka-560019, India (Phone: +91 8880377627; e-mail: drss.mech@bmsce.ac.in).

N. Ramesh Babu is with Manufacturing Engineering Section, Department of Mechanical Engineering, Indian Institute of Technology Madras, Chennai – 600036, India (e-mail: nrbabu@iitm.ac.in).

III Proposed Model for Predicting Depth of Penetration

A. Estimation of Depth of Penetration of Jet in Upper Region (hu)

Fig. 1 shows the interaction of AWJ with the target material and the geometry of kerf generated during AWJ cutting. The mechanism of material removal occurs in two different zones, i.e. upper and lower zones. As the jet traverses over the target material, an inclined kerf is generated in AWJ cutting as shown in Fig. 1. In the upper region of the kerf, abrasive particles are impacting at shallow angles with respect to the local kerf geometry. In this region, the material is removed by microcutting by free flowing abrasive particles and intergranular cracking resulted due to stress wave energy associated with shallow angles of impact. These two mechanisms occur till the local angle of impact is less than a particular critical angle (α_0) at which the erosion rate is maximum and the depth of penetration of jet at this point is 'h_u'. If the impact angle is more than this particular angle 'α_0', the erosion rate starts decreasing.

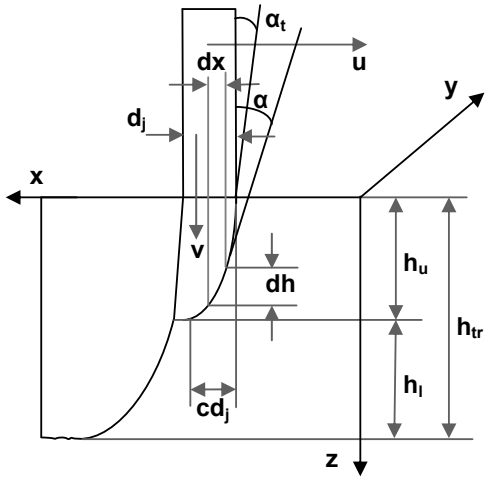

Fig. 1 Development of Geometry of Kerf

Due to the continuous traverse of jet, small steps are formed and such step formation leads to a sudden change in the curvature and abrasive particles impact the material at 90^0. These steps are removed by the particles which are impacting at 90^0. At near orthogonal impacts, the mechanism of material removal is due to plastic deformation and intergranular cracking and the depth of penetration of jet at this point is 'h_l'. To find differential abrasive mass flow rate in upper region, planar cross section of jet interacting with the target material was used [2]. This work considered an interaction of cylindrical jet with the target material in the upper region. It is given as

$$d\dot{m} \approx \frac{4\dot{m}}{\pi d_j} dx \tag{1}$$

With the consideration of cylindrical cross section of jet interacting with the target material, the volume of material removed at shallow impact angles, by free flowing abrasive particles due to cutting wear is [5]:

$$d\dot{v} = \frac{56\, \dot{m}(dx)\alpha^{1.5}}{\pi^2 \rho_p d_j} \left[\frac{V}{c_k}\right]^{2.5} \tag{2}$$

The total energy associated with the stress wave at shallow angles of impact of an abrasive particle E_s is given by [6]:

$$E_s = \frac{-10\pi(1+\nu)R_f S_f^{0.5}(\beta_3 + \beta_2\mu^2)(dm)V^2\alpha^2 H}{E} \tag{3}$$

where 'R_f' is the roundness factor of abrasive particle, 'S_f' is the sphericity of abrasive particles, the constants 'β_2' and 'β_3' depends on the Poisson's ratio 'ν' of target material [1], 'μ' is the ratio of tangential force to the normal force while microcutting, 'dm' is the differential mass of abrasive particles, 'V' is the velocity of abrasive particle at any depth 'h', 'H' is the Knoop hardness, and 'E' is the modulus of elasticity of target material. Assuming a crack network model, the volumetric MRR due to cracking which occurs due to fracture at shallow angles $d\dot{v}_{fs}$ is given by [1]:

$$d\dot{v}_{fs} = \frac{c_m f_r E_s a}{6\lambda} \tag{4}$$

where 'c_m' is the proportionality constant accounts for multiple impact, 'f_r' is the proportionality constant between the actual energy required for cracking and the stress wave energy, 'a' is an average grain size of ceramic material and 'λ' is the energy required for intergranular cracking per unit area [1]. Substituting (3) into (4), the volumetric MRR can be expressed as:

$$d\dot{v}_{fs} = \frac{-10\pi(1+\nu)R_f S_f^{0.5}(\beta_3 + \beta_2\mu^2)(d\dot{m})V^2\alpha^2 H c_m f_r a}{6\lambda E} \tag{5}$$

By substituting (1) into (5), the volumetric MRR is given as

$$d\dot{v}_{fs} = \frac{-40(1+\nu)R_f S_f^{0.5}(\beta_3 + \beta_2\mu^2)V^2\alpha^2 H c_m f_r a\dot{m}dx}{6\lambda E d_j} \tag{6}$$

The physically obtained volumetric MRR at shallow impact angles $d\dot{v}_{ts}$ is the sum of volume removed at shallow impact angles by free flowing abrasive particles due to cutting wear $d\dot{v}$ and the volumetric MRR due to cracking $d\dot{v}_{fs}$. By adding (2) and (6) physically obtained volumetric MRR at shallow impact angles $d\dot{v}_{ts}$ is given as:

$$d\dot{v}_{ts} = d\dot{v} + d\dot{v}_{fs} = \frac{56\,\dot{m}(dx)\alpha^{1.5}}{\pi^2 \rho_p d_j}\left[\frac{V}{c_k}\right]^{2.5} - \frac{40(1+v)R_f S_f^{0.5}(\beta_3+\beta_2\mu^2)V^2\alpha^2 Hc_m f_r a\dot{m}dx}{6\lambda E d_j} \quad (7)$$

The geometrically removed volumetric MRR in upper region is given by:

$$d\dot{v}_{ts} = (dh)uw = (dh)ud_j \quad (8)$$

where 'w' is width of kerf. Equating (7) to (8) and rearranging the terms:

$$\frac{dh}{dx} = \frac{56\,\dot{m}\alpha^{1.5}}{\pi^2 \rho_p u d_j^2}\left[\frac{V}{c_k}\right]^{2.5} - \frac{40(1+v)R_f S_f^{0.5}(\beta_3+\beta_2\mu^2)V^2\alpha^2 Hc_m f_r a\dot{m}}{6\lambda E u d_j^2} \quad (9)$$

To determine the impact angle of abrasives at the top of kerf (α_t), the velocity of abrasive at the top of kerf 'V_0' is assumed to be equal to the initial velocity of abrasive. Thus at h = 0, V = V_0 and $\alpha = \alpha_t$. Referring to Fig. 1, at the top of the kerf,

$$\left[\frac{dh_c}{dx}\right]_{h=0} = cot\alpha_t = \frac{1}{\alpha_t} \quad (10)$$

Substituting (10) into (9) and rearranging:

$$\frac{56\,\dot{m}}{\pi^2 \rho_p u d_j^2}\left[\frac{V}{c_k}\right]^{2.5}\alpha_t^{2.5} - \frac{40(1+v)R_f S_f^{0.5}(\beta_3+\beta_2\mu^2)V^2 Hc_m f_r a\dot{m}}{6\lambda E u d_j^2}\alpha_t^3 = 1 \quad (11)$$

The equation is of the form $x\alpha_t^{2.5} - y\alpha_t^3 = 1$, which can be numerically solved for α_t.

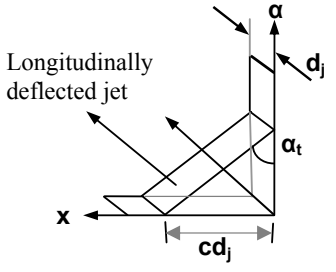

Fig. 2 Dependence of Local Angle of Attack on Geometry of Kerf

As shown in Fig. 2, the parameters 'α', 'α_t', 'x' and 'cd_j' can be related by a two-dimensional model. It is given as

$$\frac{\alpha}{\alpha_t} + \frac{x}{cd_j} = 1$$
$$\frac{\alpha}{\alpha_t} = 1 - \frac{x}{cd_j} \quad (12)$$

By differentiating (12) and rearranging the terms, we get:

$$\frac{dx}{d\alpha} = -\frac{cd_j}{\alpha_t} \quad (13)$$

where $c = \left[1 - \frac{\alpha_t}{\alpha_0}\right]$. The limiting angle for maximum erosion is 'α_0' can be expressed as,

$$(tan\alpha_0)(sin\alpha_0)^{0.5} = \frac{(3\pi R_f^{0.6})(c_K/V_0)^{0.5}}{14\gamma}$$

where $\gamma = 1 + \frac{m_p r^2}{I}$ and $I = km_p r^2$ where 'γ' is a function of the shape of abrasive particle. 'I' is the moment of inertia of the particle around its center of gravity, 'm_p' and 'r' are mass and radius of abrasive particle respectively. For spherical shaped abrasives, the inertia constant 'k' is equal to 0.5. Equation (9) is rearranged as:

$$dh = \left[\frac{56\,\dot{m}\alpha^{1.5}}{\pi^2 \rho_p u d_j^2}\left[\frac{V}{c_k}\right]^{2.5} - \frac{40(1+v)R_f S_f^{0.5}(\beta_3+\beta_2\mu^2)V^2\alpha^2 Hc_m f_r a\dot{m}}{6\lambda E u d_j^2}\right]dx$$

$$dh = \left[\frac{56\,\dot{m}}{\pi^2 \rho_p u d_j^2}\left[\frac{V}{c_k}\right]^{2.5}\alpha^{1.5}d\alpha - \frac{40(1+v)R_f S_f^{0.5}(\beta_3+\beta_2\mu^2)V^2 Hc_m f_r a\dot{m}}{6\lambda E u d_j^2}\alpha^2 d\alpha\right]\left(\frac{dx}{d\alpha}\right) \quad (14)$$

The depth of penetration of jet in the upper part of kerf achieved by microcutting and intergranular cracking at shallow angles of impact can be obtained by integrating (14) with suitable limits. The impact angle 'α' is assumed to vary from 'α_t' to 0 at the end of the upper region. The jet is deflected gradually and it becomes parallel to local kerf curvature [2]. As shown in Fig. 2, $\alpha = \alpha_t$ when x = 0. This is equivalent to $\alpha = \alpha_t$ when h = 0 and $\alpha = 0$ when $x = cd_j$ [7].

$$\int_0^{h_u} dh = \left[\frac{56\,\dot{m}}{\pi^2 \rho_p u d_j^{\,2}} \left[\frac{V}{c_k} \right]^{2.5} \int_{\alpha_t}^{0} \alpha^{1.5} d\alpha - \frac{40(1+v) R_f S_f^{\,0.5} (\beta_3 + \beta_2 \mu^2) V^2 H c_m f_r a \dot{m}}{6 \lambda E u d_j^{\,2}} \int_{\alpha_t}^{0} \alpha^2 d\alpha \right] \left(\frac{dx}{d\alpha} \right)$$

$$h_u = \left(-\frac{56 \dot{m} \alpha_t^{\,2.5}}{2.5 \pi^2 u d_j^{\,2} \rho_p} \left[\frac{V}{c_k} \right]^{2.5} + \left[\frac{40(1+v) R_f S_f^{\,0.5} (\beta_3 + \beta_2 \mu^2) V^2 H c_m f_r a \dot{m} \alpha_t^{\,3}}{18 E \lambda u d_j^{\,2}} \right] \right) \left(\frac{dx}{d\alpha} \right) \quad (15)$$

Substituting (13) into (15),

$$h_u = \left(\frac{56 c \dot{m} \alpha_t^{\,1.5}}{2.5 \pi^2 u d_j \rho_p} \left[\frac{V}{c_k} \right]^{2.5} - \left[\frac{40 c (1+v) R_f S_f^{\,0.5} (\beta_3 + \beta_2 \mu^2) V^2 H c_m f_r a \dot{m} \alpha_t^{\,2}}{18 E \lambda u d_j} \right] \right) \quad (16)$$

Equation (14) is valid only if 'c' in the above equation is positive [2], otherwise it is assumed that the total depth of penetration is achieved by plastic deformation and intergranular cracking due to near orthogonal impact.

B. Estimation of Depth of Penetration of Jet in Lower Region (hl)

In this region, the material is removed by large plastic deformation and intergranular cracking resulted due to stress wave energy associated with larger angles of impact of particles. When the jet penetrates into the material at large impact angles, the material removal occurs due to excessive plastic deformation is given by [8]:

$$d\dot{v}_p = \frac{\dot{m}}{2\sigma_f} (V - V_e)^2 \quad (17)$$

where 'σ_f' is the flow stress of target material and 'V_e' is the threshold velocity of jet. Below the threshold velocity of jet, the deformation is elastic which consumes certain energy. When the velocity of jet is lower, the role of threshold velocity seems to be significant. At higher jet velocities, role the threshold velocity in material removal can be safely neglected [9]-[11]. Neglecting the threshold velocity, the volumetric MRR due to plastic deformation at near normal impact $d\dot{v}_p$ is given by

$$d\dot{v}_p = \frac{\dot{m}}{2\sigma_f} V^2 \quad (18)$$

Volumetric MRR at normal impact of abrasive particles $d\dot{v}_{fn}$ due to stress wave energy is given as [5]:

$$d\dot{v}_{fn} = \left[\frac{5 c_m f_r}{3\lambda} \right] \left[\frac{\rho_t}{\rho_p} \right]^{0.5} \left[\frac{H}{E} \right]^{1.5} R_f^{\,1.5} S_f^{\,-0.5} a \dot{m} V^2 \quad (19)$$

where ρ_t is the density of target material. The physically obtained total volumetric MRR at near normal impact angles $d\dot{v}_{tn}$ can be obtained by adding the volumetric MRRs due to plastic deformation and stress wave energy. It is given as:

$$d\dot{v}_{tn} = \frac{\dot{m} V^2}{2\sigma_f} + \left[\frac{5 c_m f_r}{3\lambda} \right] \left[\frac{\rho_t}{\rho_p} \right]^{0.5} \left[\frac{H}{E} \right]^{1.5} R_f^{\,1.5} S_f^{\,-0.5} a \dot{m} V^2 \quad (20)$$

The geometrically obtained volumetric MRR in this mode is the product of the entire cross section area of the jet and its penetration rate (neglecting the small change in the diameter). The penetration rate is the ratio of differential height to differential time interval.

$$d\dot{v}_{tn} = \frac{\pi d_j^{\,2}}{4} \frac{dh}{dt} \quad (21)$$

By equating (20) and (21), rearranging the terms and integrating with the limits 'h_u' to 'h_{tr}' and '0' to 't', an expression for depth of penetration of jet in lower region can be obtained.

$$\int_{h_u}^{h_{tr}} dh = \left\{ \frac{\dot{m} V^2}{2\sigma_f} + \left[\frac{5 c_m f_r}{3\lambda} \right] \left[\frac{\rho_t}{\rho_p} \right]^{0.5} \left[\frac{H}{E} \right]^{1.5} R_f^{\,1.5} S_f^{\,-0.5} a \dot{m} V^2 \right\} \left[\frac{4}{\pi d_j^{\,2}} \right] \int_0^t dt \quad (22)$$

In the above equation, 't' is the time taken to remove the step and is a function of the step size and traverse speed. It is given by

$$t = \frac{step\ size}{u} = \frac{(d_j - c d_j)}{u} = \frac{(1-c) d_j}{u} \quad (23)$$

Substituting (23) into (22) and integrating, the depth of penetration in the lower part of kerf can be determined.

$$h_l = h_{tr} - h_u = \left\{ \frac{\dot{m}V^2}{2\sigma_f} + \left[\frac{5c_m f_r}{3\lambda}\right]\left[\frac{\rho_t}{\rho_p}\right]^{0.5}\left[\frac{H}{E}\right]^{1.5} R_f^{1.5} S_f^{-0.5} a\dot{m}V^2 \right\}\left[\frac{4(1-c)}{\pi d_j u}\right]$$

$$h_l = \frac{2V^2(1-c)\dot{m}}{\pi d_j u \sigma_f} + \left[\frac{20(1-c)\dot{m}c_m f_r}{3\lambda\pi d_j u}\right]\left[\frac{\rho_t}{\rho_p}\right]^{0.5}\left[\frac{H}{E}\right]^{1.5} R_f^{1.5} S_f^{-0.5} aV^2 \quad (24)$$

The total depth of penetration of jet in reinforcement material is obtained by adding (16) and (24).

$$h_{tr} = h_u + h_l = \left(\frac{56c\dot{m}\alpha_t^{1.5}}{2.5\pi^2 u d_j \rho_p}\left[\frac{V}{c_k}\right]^{2.5} - \left[\frac{40c(1+\nu)R_f S_f^{0.5}(\beta_3+\beta_2\mu^2)V^2 H c_m f_r a\dot{m}\alpha_t^2}{18E\lambda u d_j}\right]\right) + \left\{ \frac{2V^2(1-c)\dot{m}}{\pi d_j u\sigma_f} + \left[\frac{20(1-c)\dot{m}c_m f_r}{3\lambda\pi d_j u}\right]\left[\frac{\rho_t}{\rho_p}\right]^{0.5}\left[\frac{H}{E}\right]^{1.5} R_f^{1.5} S_f^{-0.5} aV^2 \right\} \quad (25)$$

TABLE I
CONSTANTS USED IN THE MODEL

Parameter	Value	Reference
Coefficient of friction on kerf wall, k_w	0.002	[7]
β_2 and β_3	1.308 and -2.7768 respectively	[1]
Effect of the multiple impact phenomenon, c_m	0.075	[2]
Overall coefficient of discharge, χ	0.83-0.93	[12]
Momentum transfer parameter, ψ	0.73-0.94	[12]
Proportionality constant between the actual energy required for cracking and the stress wave energy, f_r	$6.65*10^{-4}$	[13]
Ratio of the tangential to the normal force, μ	0.5	[12]

TABLE II
CONDITIONS EMPLOYED FOR AWJC EXPERIMENTS

Injection type AWJ Machine	By M/s WOMA, Austria of maximum pressure 360 MPa, rated discharge of 2.2 lpm and traverse speed of 0-5000 mm/min
Orifice material	Sapphire orifice of diameter of 0.25 mm
Focusing nozzle material	Tungsten carbide of diameter of 0.76 mm
Angle of impact of jet	90°
Stand-off distance	2 mm
Number of passes	1
Abrasive material	Garnet of 80 mesh size (diameter = 0.177 mm)

IV. VALIDATION OF MODEL

The experiments were conducted on SiC blocks of thickness 70 mm to determine the maximum penetration of jet into the target material. The depth of penetration was directly measured. SiC blocks were produced through powder metallurgy route with SiC particles of mesh size of 200. AWJ cutting experiments were conducted on SiC block whose density is 2800 kg/m^3, modulus of elasticity of 140 GPa, hardness of 710 kg/mm^2 (7 GPa) on Knoop scale, fracture toughness of 2.5 MPa (m)$^{0.5}$ and energy required for intergranular cracking per unit area (λ) of 22.32 J/m^2. The value chosen for λ depends upon the fracture toughness and the modulus of elasticity [1]. Threshold velocity for SiC is approximated as 184 m/s based on the data given in the literature [7]. This particular value was used to find the total depth of penetration of jet in 100% SiC block using the model proposed by Paul et al. [2]. Table I presents certain constants used in the model.

Table II presents the experimental conditions used for AWJC of SiC block. Table III shows the cutting conditions used for AWJ cutting of SiC block and the percentage error of predicted depths of penetration of jet using proposed model with experimental values. In order to show the effectiveness of the proposed model, the predicted depths of penetration of jet with the model of Paul et al. [2] and the percentage error of the predicted depths of penetration of jet with experimental values are also given.

To find the percentage error the following expression is used:

$$\%\ Error = \frac{(Experimental\ value - model\ value)100}{Experimental\ value} \quad (26)$$

From these, it can be concluded that, up to 2 mm depth of penetration, the proposed model predicted 70% higher depth of penetration than the experimental results. However, the model proposed by Paul et al. [2], predicted the depth of penetration closer to the experimentally observed values. Beyond 2 mm, Paul's model is found to give 45 to 82% error. Between 3 and 5 mm depth of penetration, the proposed model predicted depths almost closer to the experimental depths of penetration. Between 5 mm and 25 mm depths of penetration, the proposed models predicted about 20% to 45% lower depths of penetration than the experimental results. This clearly illustrates the relevance of the proposed model for predicting large depths in brittle materials.

As observed in Table III, the proposed model estimated higher depths of penetration than the experimental results up to 2 mm. This can be attributed to neglecting the threshold velocity of jet. This parameter was not considered in the model proposed by Paul et al. [2]. Thus, this observation

clearly indicates that low energy jet needed to cut thin specimen will have lower velocities and the threshold velocity should be considered in predicting these depths. At higher jet energies, the velocity of jet is much higher and its effect on material removal can be neglected.

TABLE III
CUTTING CONDITIONS AND PERCENTAGE ERROR WITH PROPOSED AND MODEL [2]

Cutting conditions	P (MPa)	$\dot{m}$ (kg/min)	u (mm/min)	Experimental	Proposed model	% Error	Model [2]	% Error
1	300	0.026	30	14	11.1	20.7	6.3	55
2	300	0.026	60	9	7.2	20	3.9	56.7
3	300	0.026	90	5.5	5.7	-3.6	3.0	45.5
4	300	0.044	30	22	15.0	31.8	8.1	63.2
5	300	0.044	60	14	10.3	26.4	5.5	60.7
6	300	0.044	90	10	7.6	24	4.2	58
7	300	0.074	30	30	20.6	31.3	11.2	62.7
8	300	0.074	60	20	13.1	34.5	7.5	62.5
9	300	0.074	90	15	10.6	29.3	5.6	62.7
10	200	0.026	30	14.5	8.2	43.4	3.8	73.8
11	200	0.026	60	8	5.5	31.3	2.4	70
12	200	0.026	90	4.5	4.2	6.7	1.8	60
13	200	0.044	30	19	11.4	40	5.1	73.2
14	200	0.044	60	13	7.5	42.3	3.4	73.8
15	200	0.044	90	9	5.9	34.4	2.6	71.1
16	200	0.074	30	25	15.0	40	6.7	73.2
17	200	0.074	60	16	9.8	38.8	4.6	71.3
18	200	0.074	90	13	7.7	40.8	3.5	73.1
19	100	0.026	30	7	5.3	24.3	1.5	78.6
20	100	0.026	60	3	3.3	-10	0.8	73.3
21	100	0.026	90	1.9	2.5	-31.6	0.5	73.7
22	100	0.044	30	11	6.9	37.3	2.0	81.8
23	100	0.044	60	5	4.6	8	1.3	74
24	100	0.044	90	2	3.4	-70	0.9	55
25	100	0.074	30	14	9.1	35	2.7	80.7
26	100	0.074	60	9	6.0	33.3	1.7	81.1
27	100	0.074	90	5	4.6	8	1.3	74

The depths of penetrations predicted in higher ranges are closer to experimental results which can be attributed to the following. (i) Consideration of the interaction of the cylindrical jet with target material can estimate more material removal rate in upper region and (ii) neglecting the role of threshold velocity can estimate more material removal rates in the lower wear region. Effectiveness of different models is evaluated by means of correlation coefficient and standard deviation (Table IV). Correlation coefficient is almost the same thus indicating the trend in deviations (Experimental value – predicted value) is the same with both the models. However, the standard deviation of the proposed model shows lesser values which in turn indicate the closeness of data points with the mean depth of penetration.

TABLE IV
STANDARD DEVIATION AND CORRELATION COEFFICIENT FOR DIFFERENT MODELS

Parameter	Proposed ceramic model	Model [2]
Standard deviation	3.10	4.79
Correlation coefficient	0.976	0.923

V. CONCLUSIONS

In this paper, a model for predicting the depth of penetration in ceramic materials is proposed. It developed a revised model for predicting the depth of penetration in ceramic materials [2] with certain modifications such as considering the interaction of cylindrical cross section of the jet in the upper region and neglecting the threshold velocity in the lower region. The effect of threshold velocity on material removal seems to be important at lower jet energies or lower depths of penetration, i.e. 2 mm. For achieving higher depths of penetration with higher energies of jet, the role of threshold velocity in material removal can safely be neglected. The results clearly indicate that the proposed model can be used to predict higher depths of penetration.

NOMENCLATURE

α	Local impact angle of the abrasive particles with respect to the kerf wall (rad)
α_0	Limiting angle at which maximum erosion occurs (rad)
α_t	Impact angle at the top of the kerf (rad)
β_2 and β_3	Functions of Poisson's ratio
χ	Overall coefficient of discharge
γ	A function of particle shape
λ	Energy required for intergranular cracking per unit area

	(J/m^2)
μ	Ratio of tangential force to the normal force while microcutting = 0.5
ν	Poisson's ratio of the target material
ψ	Momentum transfer parameter
ρ_p	Density of abrasive particle (kg/m^3)
ρ_t	Density of target material (kg/m^3)
σ_f	Flow strength of target material (N/m^2)
a	Average grain size of ceramic target material (m)
c	Constant to find partial involvement of the jet
c_k	Characteristic velocity for abrasive-material pair (m/s)
c_m	Proportionality constant taking into account the effect of multiple impact
d_j	Diameter of jet (m)
$d\alpha$	Differential impact angle (rad)
dh	Differential depth of penetration of jet into the material (m)
dh_c	Differential depth of penetration in cutting wear region (m)
h	Any depth of penetration (m)
h_c	Depth of penetration in cutting wear region (m)
h_l	Depth of penetration achieved by plastic deformation and cracking at near normal angles of impact (m)
h_t	Total depth of penetration for MMC (m)
h_{tm}	Total depth of penetration for matrix material (m)
h_{tr}	Total depth of penetration for reinforcement (m)
h_u	Depth of penetration achieved by microcutting and cracking at shallow angles of impact (m)
H	Knoop hardness of the target material (MPa)
I	Moment of inertia of the particle around its center of gravity (m^4)
k	Inertia constant = 0.5
k_w	A function of coefficient of friction and jet diameter
dm	Differential mass of abrasive particles (kg)
$d\dot{m}$	Differential mass flow rate of abrasives (kg/s)
dt	Differential time interval (s)
$d\dot{v}$	Rate of volume removal (m^3/s)
$d\dot{v}_{tn}$	Total volume removal rate at near normal impact angles (m^3/s)
$d\dot{v}_{ts}$	Total volume removal rate at shallow impact angles (m^3/s)
dv_{fn}	Volume removal at near normal impact according to crack network model (m^3)
$d\dot{v}_{fn}$	Volume removal rate at near normal impact according to crack network model (m^3/s)
$d\dot{v}_p$	volume removal rate due to plastic deformation at normal impact (m^3/s)
$d\dot{v}_{fs}$	Volume removal rate due to cracking which occurs due to fracture at shallow angles (m^3/s)
dx	Differential distance (m)
E	Modulus of elasticity of target material (GPa)
E_s	Total energy associated with the stress Wave at shallow angles of impact of an abrasive particle (J)
f_r	Proportionality constant between the actual energy required for cracking and the stress wave energy
k_1	Constant relating top and bottom width of kerf
k_2	Constant relating impact angle at the top of kerf and lateral inclination angle of jet
K_{IC}	Fracture toughness (MPa $(m)^{0.5}$)
L	Length of cut on slant surface (m)
m_p	Mass of abrasive particle (kg)
$\dot{m}$	Mass flow rate of abrasives (kg/s)
r	Radius of abrasive particle (m)
R_f	Roundness factor of abrasive particle
S_f	Sphericity of the abrasive particles
t	Time taken to remove the step (s)
V	Velocity of abrasive at h (m/s)
V_0	Velocity of the abrasives at the top of the kerf (m/s)
u	Jet traverse speed (m/s)
w	Width of kerf (m)
W_0	Stress wave energy associated with near normal impact (J)

ACKNOWLEDGMENT

Authors are thankful for the support given by Center of Excellence in Advanced Materials Research, TEQIP 1.2.1 and the Management, BMS College of Engineering in presenting this paper.

REFERENCES

[1] Jiyue Zeng and Thomas J. Kim. An erosion model of polycrystalline ceramics in abrasive waterjet cutting Wear 1996, 193, pp 207-217.
[2] Paul, S.; Hoogstrate, A.M.; Van Luttervelt, C.V.; Kals, J.J. Analytical modeling of the total depth of cut in the abrasive waterjet machining of polycrystalline brittle material. Journal of Materials Processing Technology 1998, 73, pp 206-212.
[3] Hashish, M. (1989) A model for abrasive waterjet (AWJ) machining, Transactions of ASME, Journal of Engineering Materials Technology, 111(2), 154-162.
[4] J. Wang, A new model for predicting the depth of cut in brasive waterjet contouring of alumina ceramics, journal of materials processing technology 209 (2009) pp 2314–2320.
[5] Srinivas, S.; Ramesh Babu, N. An analytical model for predicting depth of cut in abrasive waterjet cutting of ductile materials considering the deflection of jet lateral direction. International Journal of Abrasive Technology 2009 2, pp 259-278.
[6] Paul, S.; Hoogstrate, A.M.; Van Luttervelt, C.V.; Kals, J.J. Energy partitioning in elasto-plastic impact by sharp abrasive particles in the abrasive waterjet machining of brittle materials. Journal of Materials Processing Technology 1998, 73, pp 200-205.
[7] Hashish, M. A model for Abrasive waterjet (AWJ) machining. Transactions of ASME. Journal of Engineering Materials and Technology 1989, 111, pp 154-162.
[8] Bitter, J.G.A. (1963a) A study of erosion phenomena, part-I, Wear, 6, pp 5-21.
[9] Neilson, J.H.; Gilchirst, A. Erosion by a stream of particles Wear 1968, 11, pp 111-122.
[10] Hashish, M. A modeling study of jet cutting surface finish. In Precision Machining: Technology and Machine Development and Improvement. Proceedings of the Winter Annual Meeting of ASME, PED-Vol. 58, New York, Dec 1992.
[11] Vikram, G.; Ramesh Babu, N. Modelling and analysis of abrasive waterjet cut surface topography. International Journal of Machine Toolsand Manufacture 2000, 42, pp 1345-1354.
[12] Momber, A.W. and R. Kovacevic Principles of Abrasive waterjet machining, Springer-Verlag, London, 1998.
[13] Personal communications with Jay Zeng of OMAX Corporation, Kent WA 98032-1944.